

# Nonwetting, Nonrolling, Stain Resistant Polyhedral Oligomeric Silsesquioxane Coated Textiles

Rahul Misra, Robert D. Cook, Sarah E. Morgan

School of Polymers and High Performance Materials, The University of Southern Mississippi, Hattiesburg, Mississippi 39406

Received 28 December 2008; accepted 30 August 2009

DOI 10.1002/app.31365

Published online 7 October 2009 in Wiley InterScience (www.interscience.wiley.com).

**ABSTRACT:** Cotton/polyester fabric surfaces were modified using nanostructured organic-inorganic polyhedral oligomeric silsesquioxane (POSS) molecules via solution dip coating. Surface wetting characteristics of coatings prepared from two chemically and structurally different POSS molecules, a closed cage fluorinated dodecafluoropropyl POSS (FL-POSS) and an open cage nonfluorinated trisilanolphenyl POSS (Tsp-POSS), were evaluated with time and compared with Teflon. Surface analysis, including Atomic Force Microscopy, SEM/EDAX, and NMR revealed the presence of POSS aggregates on the fabric surface leading to a spiky topography, high roughness, and hysteresis. POSS coated fabrics showed complete reversal of surface wetting

characteristics with contact angles higher than the benchmark Teflon surface. Water contact angle measured as a function of time showed equivalent or better performance for POSS-coated surfaces in comparison to Teflon. Furthermore, FL-POSS coated fabric exhibited exceptional stain and acid resistance along with a 38% reduction in relative surface friction. Additionally, "nonsliding" and high surface adhesion behavior of water droplets on the FL-POSS coated fabric are reported. © 2009 Wiley Periodicals, Inc. *J Appl Polym Sci* 115: 2322–2331, 2010

**Key words:** polyhedral oligomeric silsesquioxane; fabrics; coatings; nanotechnology; atomic force microscopy

## INTRODUCTION

Advancements in nanostructured materials and coatings have sparked the development of new, multifunctional textiles. A major challenge is to develop stable nanostructured coatings that impart desired functionality, and can be applied using simple coating techniques. Nonwetting fabrics have potential utility in industrial and biomedical applications, for example to provide reduced surface friction, or resistance to staining, harsh chemicals, or bacterial activity.<sup>1,2</sup> Generally, preparation of fabric coatings that impart a high degree of hydrophobicity involves elaborate synthetic routes with stringent reaction conditions along with the use of harsh and/or expensive chemicals.<sup>3,4</sup> Recently, Cheung and coworkers<sup>5</sup> reported titanium dioxide coated self-cleaning cotton surfaces prepared via sol-gel processes. These surfaces exhibit bactericidal activity and degradation of red wine and coffee stains under UV irradiation. Similarly, Kiwi and coworkers<sup>6–8</sup> have

explored the photocatalytic activity of TiO<sub>2</sub>/SiO<sub>2</sub> coated cotton, polyesters, and wool-polyamide. The majority of the research efforts reported to date are focused on utilizing inorganic nanoparticles (TiO<sub>2</sub> and SiO<sub>2</sub>) through sol-gel chemistries. However, the high temperature required to achieve a thin layer of sol-gel based TiO<sub>2</sub> coating limits its applicability for many fabrics. There is a need to develop and expand the range of materials for coating fabric surfaces to impart multifunctionality via simple coating routes.

Polyhedral oligomeric silsesquioxane (POSS) nanostructured chemicals provide an alternate route to tailor fabric surface characteristics. POSS organic-inorganic hybrid molecules have a silicon-oxygen inorganic core surrounded by a corona of organic groups attached to corner silicon atoms. Organic groups attached to POSS cages can be readily modified to tailor the compatibility with the substrate. The inorganic cage, with structure (SiO<sub>1.5</sub>)<sub>n</sub> where *n* = 8, 10 or 12, may be a fully condensed "closed" or "open" structure. The diameter of these monodisperse molecules ranges from 1–3 nanometers depending on the composition of the cage.<sup>9</sup> Additionally, POSS molecules are environmentally benign, nontoxic, and biocompatible, and selected structures have been approved by the FDA for use in dental composite applications.<sup>10–12</sup> POSS has been widely studied in copolymers<sup>9,13–17</sup> and blends,<sup>18–20</sup> but few reports have appeared on POSS modified fabric surfaces.<sup>21</sup> Polyurethane/POSS coatings have

Correspondence to: S. E. Morgan (sarah.morgan@usm.edu).

Contract grant sponsor: STTR Program of the National Science Foundation; contract grant number: OII-0539295.

Contract grant sponsor: RET Program of the National Science Foundation; contract grant number: EEC-0602032.

been reported to improve flame retardant characteristics of textiles.<sup>22</sup> Recently, Mabry and co-workers<sup>23,24</sup> reported superhydrophobic and superoleophobic poly(methyl methacrylate) and fabric surfaces using highly hydrophobic long chain fluorodecyl and fluoroctyl POSS. Superoleophobicity was attributed to the interplay of POSS chemical composition, nanoroughened/microroughened surface texture, and re-entrant surface curvature. Although significant improvement in the hydrophobicity was reported, the researchers utilized long fluorinated chains, which are the subject of potential environmental concerns. Literature reports suggest that because of the strong C—F bond (bond dissociation energy 115 kcal/mol),<sup>25</sup> C—F chains with chain length of C8 or higher persist in the environment, bioaccumulate and have potential toxicity. Fluorocarbon chains with four or fewer carbon atoms are reported not to exhibit bioaccumulation.<sup>26</sup> Thus, further studies of short chain fluorinated POSS and nonfluorinated POSS coated fabrics are of interest.

An important characteristic of highly hydrophobic surfaces is the rolling of water droplets across the surface without wetting or adhesion, enabling self-cleaning properties. However, this also leads to poor adhesion and dyeability, limiting the utility of the fabric. For many applications, it is equally important to maintain low surface friction. Recently, we have demonstrated significantly improved surface hydrophobicity and frictional characteristics of melt blended POSS/polymer composites.<sup>27,28</sup> In this work, short chain fluorinated and nonfluorinated POSS nanostructured chemicals are employed to manipulate surface wetting characteristics of fabrics via simple solution dip coating. An attempt is made to understand and evaluate the effect of POSS coating on fabric surface friction, hydrophobicity, and resistance to stain and acid. In addition, nonsliding and high surface adhesion behavior at different tilt angles is discussed.

## EXPERIMENTAL

### Materials

A laboratory grade polyester/cotton blend (65 : 35 by wt. ratio) fabric was purchased from Landau Uniforms, (Memphis, TN). A closed cage fluorinated dodecatrifluoropropyl POSS (FL-POSS) and an open cage nonfluorinated trisilanolphenyl POSS (Tsp-POSS) were provided by Hybrid Plastics, (Hattiesburg, MS). POSS samples (Fig. 1) were received as crystalline white powder at room temperature and used as received. Per the supplier's analysis, the POSS samples were pure, monotonic in cage size, and contain no oligomers. Polytetrafluoroethylene (Teflon) film was provided by DuPont (Cirleville,

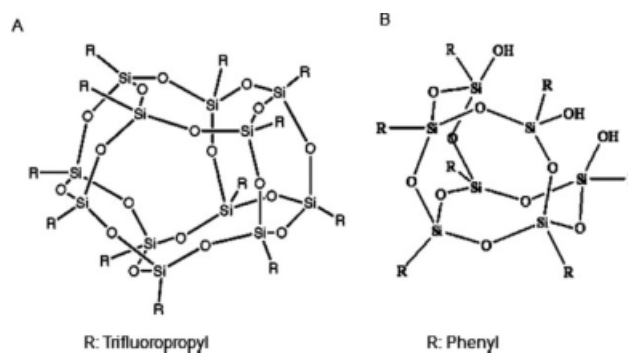


**Figure 1** Molecular structure of A: FL- POSS, B: Tsp-POSS.

OH). Silicon wafers were purchased from Silicon, Inc., and cut into 1 × 2 cm pieces using a diamond-tipped glass cutter.

### Sample preparation

To remove any external contaminants, fabric was washed with soap (mixture of ammonium and sodium lauryl sulfate) followed by thorough rinsing with water and drying in air. Cleaned and dried fabric was dipped in 10 wt % solution of POSS in tetrahydrofuran (THF) for 12 hrs followed by drying under hood for 4–5 hrs. For surface characterization, a small piece of fabric was cut and attached to a glass slide using a double sided tape.

In an attempt to estimate thickness of the POSS coatings, POSS solutions were deposited on silicon wafers using the same procedure as that used for the fabric coatings. Silicon wafers were cleaned using piranha solution (30 : 70 v/v solution of 30% hydrogen peroxide and concentrated sulfuric acid). The solution was heated for 2 h at 100°C. *Caution: piranha solution is extremely caustic.* Wafers were cleaned in HPLC water, ethanol and HPLC water sequentially before immersion in POSS solutions.

### Atomic force microscopy (AFM) surface topography

Surface topography studies were conducted on a MultiMode<sup>TM</sup> scanning probe microscope from Veeco Instruments, (Santa Barbara, CA). Probes for surface studies were purchased from Veeco Probes, (Santa Barbara, CA). A silicon probe with a 125 μm long silicon cantilever, nominal force constant of 40 N/m, and resonance frequency of 275 kHz was used for tapping mode surface topography studies. AFM studies were conducted under ambient conditions in a temperature (27°C) and humidity controlled (40–45%) room. All samples were stored in a humidity controlled chamber, and measurements were conducted in the same day to minimize environmental

effects. Surface topography was studied on a  $2\ \mu\text{m} \times 2\ \mu\text{m}$  scan area with an image resolution of  $512 \times 512$  pixels at a scan rate of 1 Hz. Multiple areas were imaged and figures show representative morphology. Surface roughness analysis was performed using Nanoscope version 5.30 r2 image analysis software.

#### Nanoindentation film thickness measurements

Nanoindentation thickness evaluations were performed on a Hysitron TriboIndenter<sup>®</sup> with a three sided diamond pyramid (Berkovich Type) tip using Triboscan<sup>®</sup> 6.0 image analysis software, following a previously reported procedure.<sup>29</sup> Tip calibration was performed using fused silica as the reference material. Normal force was applied to the surface at a loading and unloading rate of  $10\ \mu\text{N}/\text{sec}$  with a ten second hold period between loading and unloading cycle. Nanoindentation was performed under closed loop with load control using compliance method in which force-displacement curves are obtained during loading and unloading cycles. As the indenter presses into the surface the displacement is recorded as a function of the applied load. Thickness of the POSS film was determined from the change in slope in the force-distance curve.

#### Scanning electron microscopy-Energy dispersive X-ray (SEM-EDAX)

Morphology of the fabric samples was investigated using FEI Quanta 200 Scanning Electron Microscope (SEM) in high voltage mode, equipped with a Thermo-Noran Vantage light element energy dispersive X-ray detector. Before imaging, samples were sputter-coated with gold (5 nm thickness) to avoid damage to the fabric surface. Characterization of all the elements except hydrogen was obtained by X-ray spectroscopy under electron flux at a voltage of 25 kV and 1 torr pressure.

#### Proton (<sup>1</sup>H) NMR studies

A Varian 200 MHz NMR equipped with a standard 5 mm <sup>1</sup>H/<sup>13</sup>C probe was used to identify the presence of POSS on the fabric. FL-POSS coated fabric was dipped in deuterated chloroform (CDCl<sub>3</sub>) solution for 10–15 min to extract POSS deposited on the fabric surface. Note that while the POSS samples are soluble in both THF and chloroform, deuterated chloroform was employed for the NMR studies as deuterated THF was not readily available. For reference purposes, <sup>1</sup>H NMR spectra of FL-POSS and neat fabric were also taken following a similar procedure. <sup>1</sup>H NMR spectra of all the

samples were obtained from 256 scans with a relaxation delay of 1 sec.

#### Surface hydrophobicity and hysteresis evaluation

Surface wetting characteristics of fluorinated and nonfluorinated POSS coated fabrics were evaluated by measuring static contact angle on the fabric surface. Measurements were conducted using the sessile drop technique by a ramè-hart goniometer coupled with DROPimage<sup>®</sup> data analysis software. Ten  $\mu\text{L}$  of water was dropped onto a flat fabric surface and contact angle was measured after every 5 min over a period of 30 min. For comparison purposes, a similar test was performed on the Teflon film surface (note that this is the flat film, not Teflon coated fabric). Five measurements were taken across the surface, and an average value is reported. Adhesion of water droplets onto POSS coated fabric was observed by capturing an image of the water drop on the fabric surface at different tilt angles. Hysteresis was measured via dynamic contact angle measurements. Advancing and receding contact angles were measured, and their difference reported.

#### Stain and acid-resistance

To evaluate the stain-resistance of FL-POSS coated fabric, a few drops (10–12  $\mu\text{L}$  each) of coffee (Folgers<sup>®</sup> medium roast drip coffee) was placed on the fabric surface through a microsyringe. Spreading of fluids was monitored visually by capturing the pictures through a digital camera at the beginning and after 10 min. The stain area was observed visually by sucking back the fluid drops by a microsyringe. Similarly, acid-resistance was evaluated by putting drops of concentrated sulfuric acid on the FL-POSS coated fabric. Spreading of acid drops, their permeation beneath the fabric surface, and stain area were also monitored visually by capturing digital pictures at the beginning and after 20 sec time. For comparison purposes, similar tests were also conducted on neat fabric.

To obtain an estimate of the porosity of the POSS films, FL-POSS coated silicon wafers were imaged by AFM before and after treatment with coffee, and the RMS roughness evaluated.

#### Friction evaluation

Dynamic coefficient of friction (COF) measurements were performed according to ASTM G 99, using a pin-on-disk tribometer (Micro Photonics, PA). Two sets of readings were taken for each sample (1"  $\times$  1") inside a controlled humidity chamber (40% relative humidity) at 27°C. FL-POSS coated fabric samples were mounted firmly on a flat metal disc, which

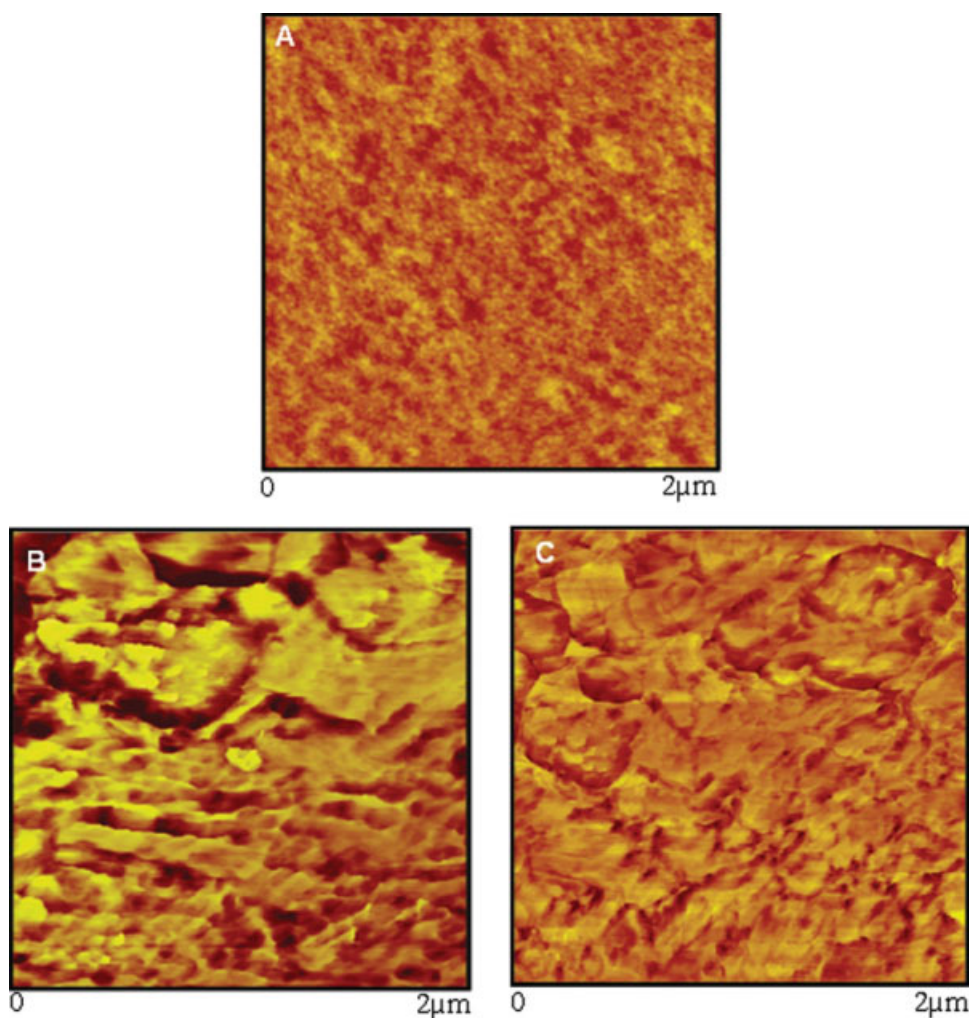


**Figure 2** AFM Phase image of A: neat fabric (Z scale:10°), B: Tsp-POSS coated fabric (Z scale:100°), C: FL-POSS coated fabric (Z scale:100°). [Color figure can be viewed in the online issue, which is available at [www.interscience.wiley.com](http://www.interscience.wiley.com).]

was rotated (path radius 3 mm) against a steel ball (3 mm diameter, Small Parts, Miami Lakes, FL) at 20 rpm for 20 min. Relative surface friction measurements were conducted at an external load of 4N.

#### Thermogravimetric analysis (TGA)

Chemical composition (polyester to cotton ratio) and thermal stability of neat and FL-POSS coated fabric samples were evaluated by thermogravimetric analysis utilizing a TA series Q500 instrument. Approximately 10–15 mg of fabric sample was used for analysis. Percentage weight loss of each sample was recorded on a platinum pan as a function of temperature from a starting temperature of 35°C up to 700°C, at a rate of 10°C per minute under 60 mL/min nitrogen purge rate.

## RESULTS AND DISCUSSION

Tapping mode AFM phase images and 3D surface topography of neat and POSS coated fabric are

shown in Figures 2 and 3, respectively. Incorporation of POSS significantly alters the fabric surface topography with the appearance of large, raised features (150–200 nm in diameter, up to 100 nm in height) on the surface. These features were identified as POSS aggregates through multiple tools, including surface roughness, NMR, SEM-EDAX, and contact angle measurements as discussed in later sections. Table I shows the influence of POSS coating on the surface roughness profile. Neat fabric appears relatively smooth (root mean square roughness, RMS, of 0.6 nm), whereas Tsp-POSS and FL-POSS coated fabrics exhibit 12 and 20-fold increase in surface roughness, respectively. To obtain an indication of the thickness of the POSS coating on the fabric surface, POSS films were prepared on silicon wafers following the fabric coating procedures. Film thickness measured by nanoindentation ranged from 70–110 nm. As the magnitude of the surface roughness features is similar to that of the measured film thickness, it is likely that the POSS coating thickness is not uniform across the fabric surface.

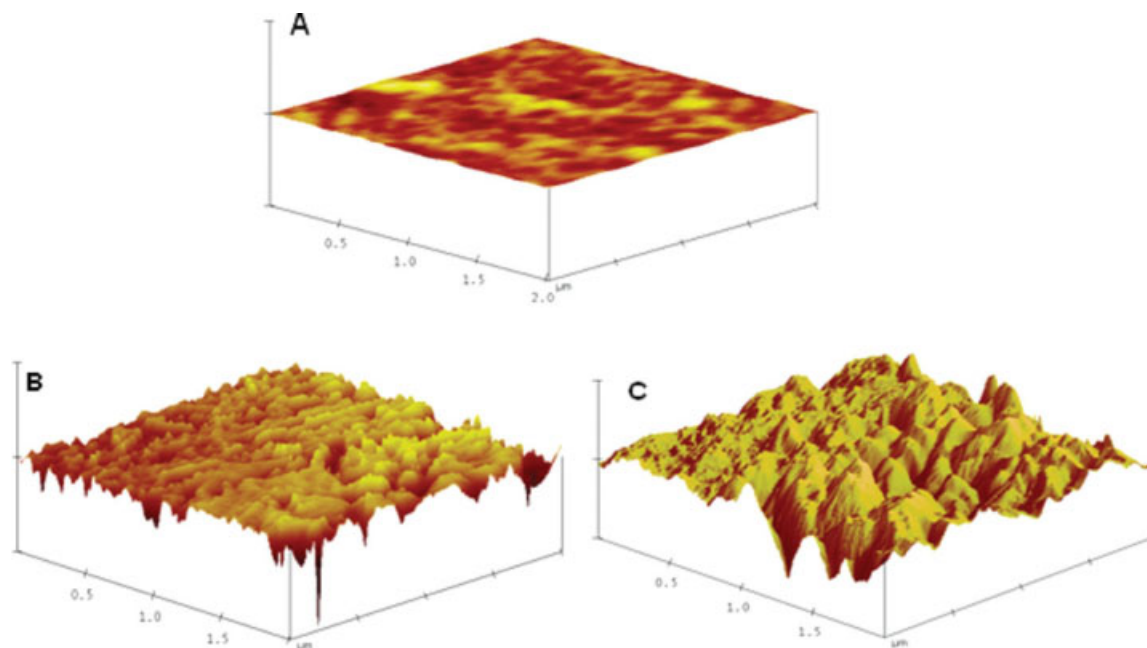


**Figure 3** Three dimensional surface topography of A: neat fabric, B: Tsp-POSS coated fabric, C: FL-POSS coated fabric (Z scale: 100 nm). [Color figure can be viewed in the online issue, which is available at [www.interscience.wiley.com](http://www.interscience.wiley.com).]

SEM micrographs and corresponding EDAX elemental analysis of neat and FL-POSS-coated fabrics are shown in Figure 4(A,B). Uniform spherical surface features (100–150 nm) are observed on the POSS coated fabric. EDAX elemental analysis identifies these features as POSS aggregates, because of the appearance of the signature peak of silicon atom at 1.7 KeV. Additional peaks at 0.7 and 2.2 KeV are attributed to fluorine (from the trifluoropropyl substituents on FL-POSS) and gold (from the gold sputtering), respectively.

Recognizing the fact that SEM/EDAX probes the surface a few microns deep (3–4  $\mu\text{m}$ ), proton ( $^1\text{H}$ ) NMR studies were conducted to evaluate the chemical nature of the surface features by extracting them from the fabric surface in  $\text{CDCl}_3$  solvent. Figure 5 shows the NMR spectra of the FL-POSS, solvent, and neat and FL-POSS coated fabrics.  $^1\text{H}$  NMR spectra of neat fabric shows a singlet due to the presence of moisture in the solvent, whereas neat POSS exhibits two triplets at 2.3 and 1.1 ppm which are attributed to: (a) the protons in proximity to the fluorine atoms and (b) two protons which are close to the silicon atoms. The presence of these two characteristic triplet peaks in the spectra of the coated fabric indicates the presence of POSS on the fabric surface.

Conventionally, fluorinated additives and coatings are employed to impart hydrophobicity to surfaces, so it is of interest to evaluate the wetting characteristics of nonfluorinated POSS coated fabrics as well. Instant spreading of a water droplet on the uncoated fabric indicates its highly hydrophilic nature. Incorporation of POSS in the fabric results in a dramatic

increase in the surface hydrophobicity. Table II shows the water contact angle analysis with time for fluorinated and nonfluorinated POSS coated fabrics in comparison with that of a relatively flat Teflon film surface. The POSS-coated fabric surfaces exhibit contact angles of  $120^\circ$  to  $137^\circ$ , indicating reversal of surface wetting character. Interestingly, POSS coated fabrics exhibited higher hydrophobicity than the benchmark hydrophobic Teflon film surface. The FL-POSS coated fabric exhibits a contact angle of  $137^\circ$ , approaching superhydrophobic behavior. Multiple factors, including high surface roughness, spiky morphology caused by the presence of POSS aggregates coupled with the hydrophobic fluorinated organic groups of FL-POSS contribute to the high hydrophobicity. This behavior is in agreement with the recent findings reported by Mabry and co-workers<sup>23,24</sup> on the superoleophobic and superhydrophobic fabric surfaces using highly hydrophobic long chain fluorodecyl and fluoroctyl POSS.

Contact angle measurements as a function of time provide an indication of the stability of the surface

**TABLE I**  
AFM Roughness Analysis on Neat and POSS Coated Fabrics

Sample	Mean roughness (nm)	RMS roughness (nm)	Max. height (nm)
Neat fabric	0.5	0.6	4.8
Tsp-POSS coated fabric	5.4	7.3	55.6
FL-POSS coated fabric	10.5	13.9	114

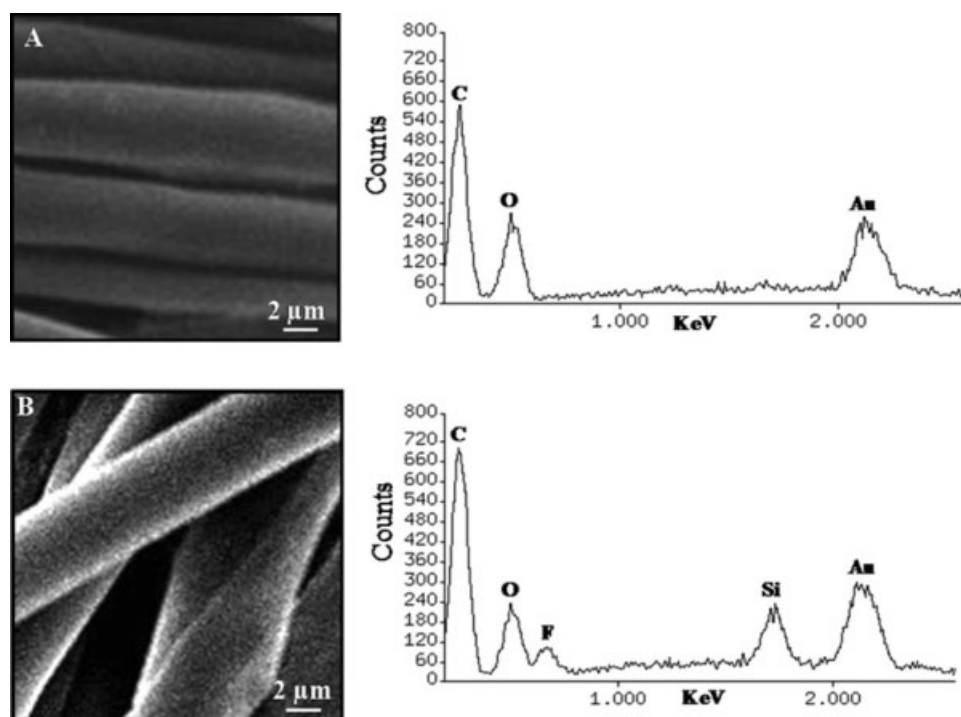


**Figure 4** SEM micrograph and corresponding EDAX map of A: neat fabric, B: FL-POSS coated fabric.

hydrophobicity. All surfaces exhibited some extent of reduction in contact angles with time. Among the two POSS molecules evaluated, FL-POSS exhibited the most stable nonwetting characteristics over the evaluated time period (9% drop in contact angle for FL-POSS vs 50% drop for Tsp-POSS). The Teflon film surface exhibited a 30% drop in contact angle over the same time period. It is important to note that the overall reduction in water contact angle over time is a combined effect of evaporation and spreading of the water droplet. Spreading is mainly characterized by reduction in the height of the water droplet with simultaneous increase in its width. Evaporation, on the other hand, is characterized by

reduction in both height and width of the water droplet. Figure 6 shows the simultaneous reduction in the height and width of a water droplet on a Teflon surface over time. POSS coated fabric surfaces exhibited contact angle reduction caused primarily by the evaporation over 30 min, similar to the behavior exhibited by Teflon film. More importantly, all surfaces exhibited original levels of high hydrophobicity after drying.

Commonly, highly hydrophobic surfaces exhibit rolling of a water droplet because of poor adhesion between the solid-liquid interface and limited hysteresis.<sup>23</sup> In our samples, nonsliding (Wenzel state)<sup>30</sup> behavior of water droplets on POSS coated fabric was observed even after tilting the surface by 180°. Figure 7 shows the pinning of a water droplet onto the FL-POSS coated fabric surface at different tilt angles, indicating high adhesion at the fabric-water interface. Hysteresis measurements (Table III) exhibit

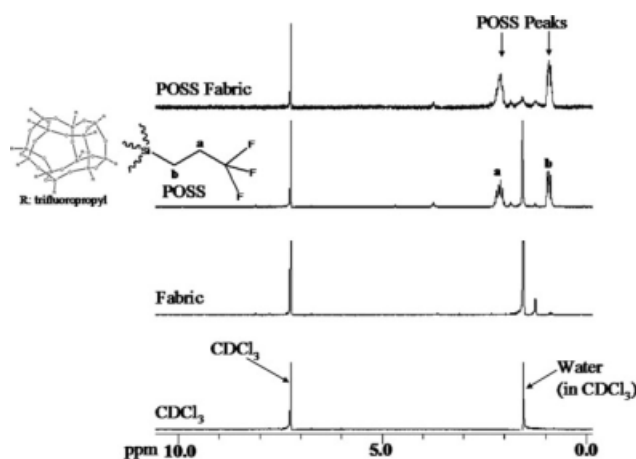


**Figure 5** Proton NMR showing the presence of POSS on FL-POSS coated fabric.

**TABLE II**  
Comparative Static Water Contact Angle Analysis for  
POSS Coated Fabrics and Teflon

Time (min)	FL-POSS (°)	Tsp-POSS (°)	Teflon (°)
0	137	119	112
1	136	118	111
2	136	117	109
5	136	116	103
10	134	113	98
15	134	110	95
20	133	100	91
25	132	86	80

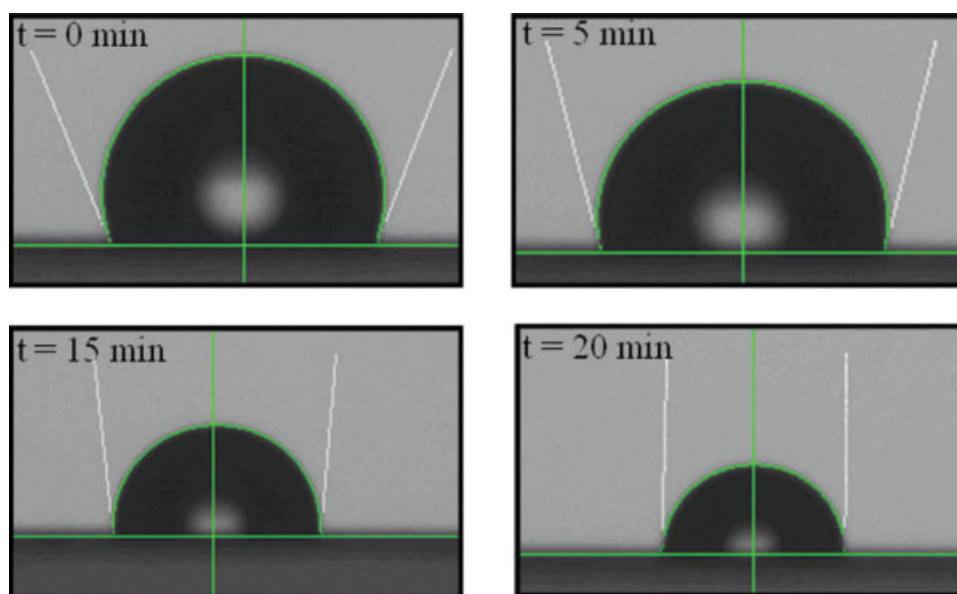


**Figure 6** Variation in the size of water droplet with time on tefflon film surface. [Color figure can be viewed in the online issue, which is available at [www.interscience.wiley.com](http://www.interscience.wiley.com).]

a large difference between the advancing and receding contact angles, indicating a chemically heterogeneous and highly rough surface. POSS coated fabric exhibited high hysteresis, which, in part, explains the nonsliding behavior of the water droplet at different tilt angles. Recently Xu and coworkers<sup>31</sup> reported a similar ultrahydrophobic and nonsliding behavior of poly (methyl methacrylate) and amphiphilic polyurethane (hydrophilic polyethylene glycol and hydrophobic fluorinated isocyanate blocks) blend surfaces. Multiple studies on droplet sliding behavior and control of the Cassie/Wenzel transition have appeared for nanopatterned surfaces, which indicate that the size and the separation of the nanoscale hydrophobic features are important in determining wetting behavior.<sup>32–35</sup> In the POSS coated fabrics, high hydrophobicity is attributed to the increased surface roughness and the presence of low surface energy, hydrophobic POSS domains on the surface. It is likely that the hydrophobic POSS domains are not continuous across the surface, but rather coexist with small hydrophilic fabric domains, which allow wetting between the hydrophobic elements and sticking of the water droplets.

In addition to the increase in hydrophobicity, stain resistance of the FL-POSS coated fabric, as tested with a coffee droplet, shows significant improvement. Figure 8(A,B) clearly shows that the coffee droplet spreads instantly on the uncoated fabric leading to a large stain area, whereas minimal spreading is observed for the POSS-coated fabric even after 10 min. After removing the coffee droplet from the coated fabric surface, significant reduction in the stain area is observed [Fig. 8(C)]. AFM analysis of the FL-POSS coated silicon wafer showed no

change in surface morphology or measured roughness on treatment with coffee, indicating the robustness of the FL-POSS coating. The Tsp-POSS coated silicon wafer, on the other hand, showed dramatic increase in roughness and development of large pores on treatment with coffee. FL-POSS coated fabric also showed improved acid resistance, evaluated with a drop of concentrated sulfuric acid [Fig. 9(A,B)]. In the case of acid spillage, exposure time is critical and a quick response (within a few seconds)

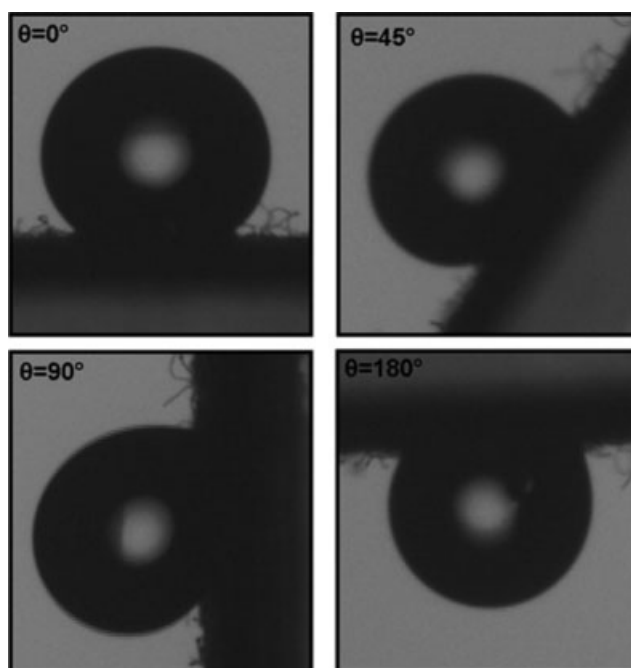


**Figure 7** Adhesion of water droplet onto FL-POSS coated fabric at varying tilt angles.

**TABLE III**  
Contact Angle Hysteresis for POSS Coated Fabrics

Sample	Advancing ( $\theta_a$ ) ( $^\circ$ )	Receding ( $\theta_r$ ) ( $^\circ$ )	Hysteresis ( $^\circ$ )
FL-POSS coated fabric	147	120	27
Tsp-POSS coated fabric	128	110	18

is required to minimize the damage to the exposed area. Although neat fabric showed instant spreading and permeation of acid to the surface beneath it, POSS-coated fabric offered significant resistance to spreading as well as permeation. Figure 9(B) shows

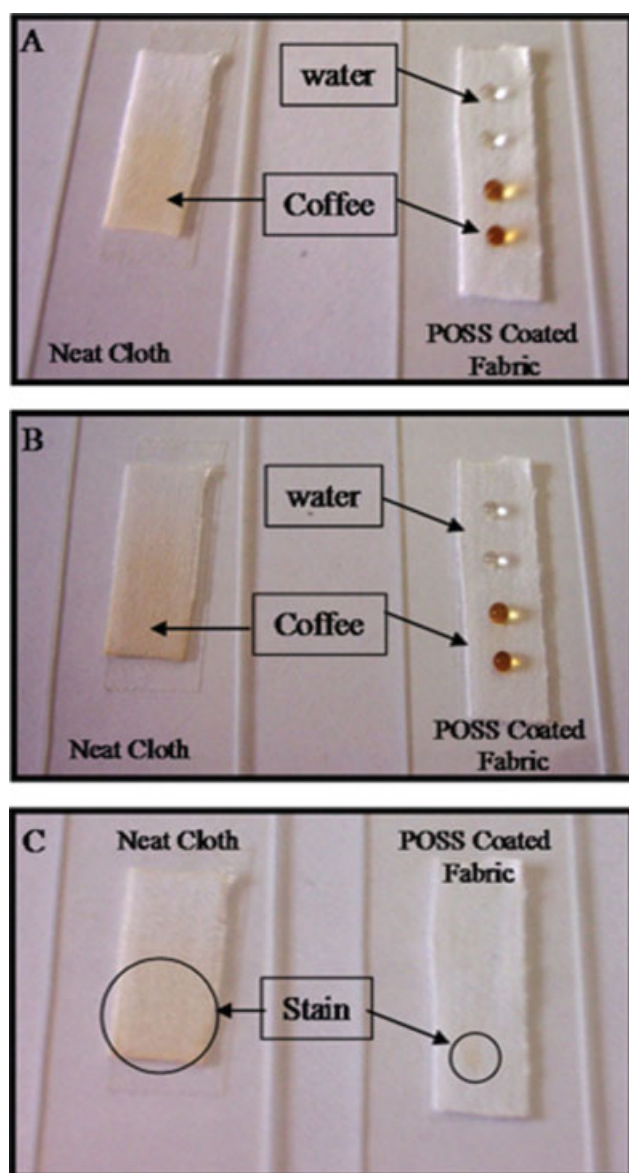


**Figure 8** Effect of water and coffee droplet on neat and FL-POSS coated fabric A: time  $t = 0$ , B:  $t = 10$  min, C: comparison of stain area after removal of coffee droplets. [Color figure can be viewed in the online issue, which is available at [www.interscience.wiley.com](http://www.interscience.wiley.com).]

that a relatively small amount of acid permeates to the reverse side of the fabric after 20 seconds, significantly reducing the exposure to the surface beneath it. Enhanced stain and acid resistance are attributed to the enhanced surface roughness and presence of chemically robust FL-POSS cages on the surface.

A significant reduction in relative surface friction is exhibited on fabrics coated with FL-POSS. Figure 10 shows the relative surface friction for neat and FL-POSS treated samples. FL-POSS coated fabric exhibits a friction coefficient of 0.08 in comparison with 0.13 for neat fabric, a 38% reduction in surface friction. Reduction in relative surface friction is attributed to the presence of POSS aggregates on the surface, as has been observed in previous studies of POSS/polymer blends.<sup>27,28</sup> Additionally, increased surface roughness, which reduces the true area of contact between the sliding surfaces, contributes to reduction in measured surface friction.

Finally, to understand the influence of POSS coating on the thermal stability and decomposition behavior of fabric, thermogravimetric analysis was performed. Both neat and FL-POSS coated fabrics exhibited a stepwise decomposition behavior with the cotton component decomposing first at lower

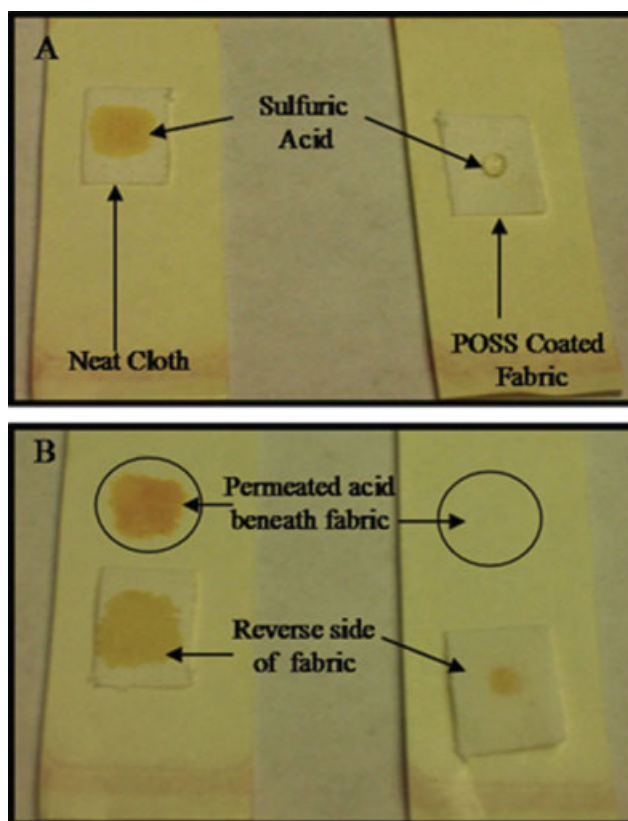


**Figure 9** Acid resistance of neat and FL-POSS coated fabric at A: time  $t = 0$ , B:  $t = 20$  sec. [Color figure can be viewed in the online issue, which is available at [www.interscience.wiley.com](http://www.interscience.wiley.com).]



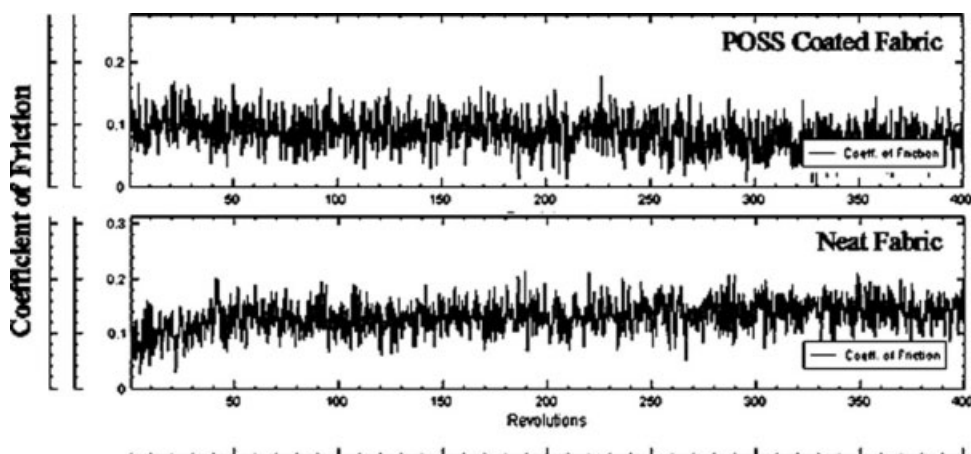


Figure 10 Relative friction coefficient of neat and FL-POSS coated fabric.

temperatures (peak degradation temperature,  $T_p = 409^\circ\text{C}$ ) followed by the decomposition of the polyester component at higher temperatures ( $T_p = 478^\circ\text{C}$ ). Percentage weight loss at the step change is linked to the composition of the fabric, with 35% weight loss at the first degradation peak indicating 35% cotton and 65% polyester, equivalent to the composition reported by the supplier. Furthermore, TGA thermograms show no affect of the POSS coating on the thermal stability of the fabric over the entire temperature range.

## CONCLUSIONS

This study demonstrates the reversal of the surface wetting characteristics of a hydrophilic fabric via nanostructured coating of organic-inorganic POSS molecules. The presence of POSS aggregates on the coated fabric surface, confirmed via AFM, NMR, and SEM/EDAX, leads to a spiky topography with 12 to 20-fold increases in surface roughness. Short chain FL-POSS molecules exhibited highly stable, nonwetting characteristics, approaching superhydrophobic behavior on a hydrophilic fabric surface. Interestingly, nonfluorinated Tsp-POSS coated fabric showed nonwetting behavior at a level that is typically exhibited by fluorinated materials. Stability of the POSS-induced hydrophobicity as a function of exposure to water over time was similar to that observed for Teflon. More importantly, drying of the POSS-coated surfaces after exposure to water resulted in a return to initial levels of hydrophobicity. Further studies of the effects of washing cycles on hydrophobicity are a subject of ongoing research efforts in our laboratory. The chemical composition of the POSS molecules coupled with their surface morphology and roughness profiles explain their hydrophobic effects.

Typically, water droplets roll on highly hydrophobic surfaces, because of limited hysteresis and adhe-

sion. However, in our studies, POSS coated surfaces exhibited high hydrophobicity coupled with high hysteresis and nonsliding behavior of water droplets even after tilting the surface by  $180^\circ$ . This behavior is attributed to the nonhomogeneous, nanoroughened surface, that allows "sticking" of the water droplets to the hydrophilic fabric substrate, while the coating of low surface energy, hydrophobic POSS domains on the surface simultaneously promotes hydrophobicity.

Additionally, FL-POSS coated fabric exhibited exceptional stain and acid resistance along with a significant reduction in relative surface friction. The nanoroughened surface and performance improvements resulted from a simple dip-coating process. This study indicates potential to develop environment friendly and cost effective nonfluorinated POSS-based coatings through effective control of surface morphology and POSS chemistry.

The authors thank Hybrid Plastics Inc., (Hattiesburg, MS) for providing POSS materials.

## References

1. Nakajima, A.; Hashimoto, K.; Watanabe, T. *Monatsh Chem* 2001, 132, 31.
2. Coulson, S. R.; Woodward, I.; Badyal, J. P. S.; Brewer, S. A.; Willis, C. *J Phys Chem B* 2004, 104, 8836.
3. Lau, K. K. S.; Bico, J.; Teo, K. B. K.; Chhowalla, M.; Amaratunga, G. A. J.; Milne, W. I.; McKinley, G. H.; Gleason, K. K. *Nano Lett* 2003, 3, 1701.
4. Erbil, Y. H.; Demirel, L. A.; Avci, Y.; Mert, O. *Science* 2003, 299, 1377.
5. Qi, K.; Walid, A. D.; Xin, J. H.; Mak, C. L.; Tang, W.; Cheung, W. P. *J Mater Chem* 2006, 16, 4567.
6. Yuranova, T.; Mosteo, R.; Bandara, J.; Laub, D.; Kiwi, J. *J Mol Catal A Chem* 2006, 244, 160.
7. Meilert, K. T.; Laub, D.; Kiwi, J. *J Mol Catal A Chem* 2005, 237, 101.
8. Bozzi, A.; Yuranova, T.; Kiwi, J. *J Photochem Photobiol Chem* 2005, 172, 27.
9. Lichtenhan, J. D. *Comments Inorg Chem* 1995, 17, 115.

10. Fong, H.; Dickens, S. H.; Flaim, G. M. *Dental Mater* 2005, 21, 520.
11. Dodiuk-Kenig, H.; Maoz, Y.; Lizenboim, K.; Eppelbaum, I.; Zalsman, B.; Kenig, S. J. *Adhes Sci Technol* 2006, 20, 1401.
12. Klapdohr, S.; Moszner, N. *Chem Mon* 2005, 136, 21.
13. Shockey, E. G.; Bolf, A. G.; Jones, P. F.; Schwab, J. J.; Chaffee, K. P.; Haddad, T. S.; Lichtenhan, J. D. *Appl Organomet Chem* 1999, 13, 311.
14. Lee, A.; Lichtenhan, J. D. *J Appl Polym Sci* 1999, 73, 1993.
15. Romo-Uribe, A.; Mather, P. T.; Haddad, T. S.; Lichtenhan, J. D. *J Polym Sci Part B: Polym Phys* 1998, 36, 1857.
16. Patel, R. R.; Mohanraj, R.; Pittman, C. U. *J Polym Sci Part B: Polym Phys* 2006, 44, 234.
17. Lee, A.; Lichtenhan, J. D. *Macromolecules* 1998, 31, 4970.
18. Ning, H.; Martin, B.; Andreas, S. *Macromolecules* 2007, 40, 9672.
19. Fu, B. X.; Hsiao, B. S.; Pagola, S.; Stephens, P.; White, H.; Rafailovich, M.; Sokolov, J.; Mather, P. T.; Jeon, H. G.; Phillips, S.; Lichtenhan, J. D.; Schwab, J. *Polymer* 2001, 42, 599.
20. Zhao, Y.; Schiraldi, D. A. *Polymer* 2005, 46, 11640.
21. Tuteja, A.; Choi, W.; Mabry, J. M.; Mckinley, G. H.; Cohen, R. E. *Proc Natl Acad Sci USA* 2008, 105, 18200.
22. Eric, D.; Maryline, R.; Serge, B. *Fire Mater* 2002, 26, 149.
23. Tuteja, A.; Choi, W.; Ma, M.; Mabry, J.; Mazzella, S.; Rutledge, G.; Mckinley, G.; Cohen, R. E. *Science* 2007, 318, 1618.
24. Mabry, J. M.; Yandek, G. R.; Haddad, T. S.; Moore, B. M.; Mcgrath, L. M.; Ruth, P. N. *ACS Polym Prepr* 2008, 49, 872.
25. Blanksby, S. J.; Ellison, G. B. *Acc Chem Res* 2003, 36, 255.
26. Available at: [http://pubs.acs.org/subscribe/journals/esthag-w/2005/nov/tech/rr\\_reformulating.html](http://pubs.acs.org/subscribe/journals/esthag-w/2005/nov/tech/rr_reformulating.html)
27. Misra, R.; Fu, B. X.; Morgan, S. E. *J Polym Sci Part B: Polym Phys* 2007, 45, 2441.
28. Misra, R.; Fu, B. X.; Plagge, A.; Morgan, S. E. *J Polym Sci Part B: Polym Phys* 2009, 47, 1088.
29. Misra, R.; Li, J.; Cannon, G. C.; Morgan, S. E. *Biomacromolecules* 2006, 7, 1463.
30. Wenzel, R. N. *J Ind Eng Chem* 1936, 28, 988.
31. Zhao, N.; Xie, Q.; Kuang, X.; Wang, S.; Li, Y.; Lu, X.; Tan, S.; Shen, J.; Zhang, X.; Zhang, Y.; Xu, J.; Han, C. *Adv Funct Mater* 2007, 17, 2739.
32. Yeh, K.-Y.; Cho, K.-H.; Chen, L.-J. *Langmuir* 2009, Article ASAP DOI: 10.1021/la9015492
33. Balu, B.; Kim, J. S.; Breedveld, V.; Hess, D. W. *J Adhes Sci Tech* 2009, 23, 361.
34. Bahadur, V.; Garimella, S. V. *Langmuir* 2009, 25, 4815.
35. Yoshimitsu, Z.; Nakajima, A.; Watanabe, T.; Hashimoto, K. *Langmuir* 2002, 18, 5818.